Joint Face Detection and Alignment Using Multitask Cascaded Convolutional Networks

Kaipeng Zhang, Zhanpeng Zhang, Zhifeng Li, Senior Member, IEEE, and Yu Qiao, Senior Member, IEEE

Abstract—Face detection and alignment in unconstrained environment are challenging due to various poses, illuminations, and occlusions. Recent studies show that deep learning approaches can achieve impressive performance on these two tasks. In this letter, we propose a deep cascaded multitask framework that exploits the inherent correlation between detection and alignment to boost up their performance. In particular, our framework leverages a cascaded architecture with three stages of carefully designed deep convolutional networks to predict face and landmark location in a coarse-to-fine manner. In addition, we propose a new online hard sample mining strategy that further improves the performance in practice. Our method achieves superior accuracy over the stateof-the-art techniques on the challenging face detection dataset and benchmark and WIDER FACE benchmarks for face detection, and annotated facial landmarks in the wild benchmark for face alignment, while keeps real-time performance.

Index Terms—Cascaded convolutional neural network (CNN), face alignment, face detection.

I. INTRODUCTION

ACE detection and alignment are essential to many face applications, such as face recognition and facial expression analysis. However, the large visual variations of faces, such as occlusions, large pose variations, and extreme lightings, impose great challenges for these tasks in real-world applications.

The cascade face detector proposed by Viola and Jones [2] utilizes Haar-Like features and AdaBoost to train cascaded classifiers, which achieves good performance with real-time efficiency. However, quite a few works [1], [3], [4] indicate that this kind of detector may degrade significantly in real-world applications with larger visual variations of human faces even with more advanced features and classifiers. Besides the cas-

Manuscript received April 7, 2016; revised June 12, 2016 and July 31, 2016; accepted August 10, 2016. Date of publication August 26, 2016; date of current version September 9, 2016. This work was supported in part by External Cooperation Program of BIC, in part by Chinese Academy of Sciences (172644KYSB20160033, 172644KYSB20150019), in part by Shenzhen Research Program under Grant KQCX2015033117354153, Grant JSGG20150925164740726, Grant CXZZ20150930104115529, Grant CYJ20150925163005055, and Grant JCYJ201 60510154736343, in part by Guangdong Research Program under Grant 2014B050505017 and Grant 2015B010129013, in part by the Natural Science Foundation of Guangdong Province under Grant 2014A030313688, and in part by the Key Laboratory of Human Machine Intelligence-Synergy Systems through the Chinese Academy of Sciences. The associate editor coordinating the review of this manuscript and approving it for publication was Dr. Alexandre X. Falcao.

K. Zhang, Z. Li, and Y. Qiao are with Shenzhen Institutes of Advanced Technology, Chinese Academy of Sciences, Shenzhen 518055, China (e-mail: kp.zhang@siat.ac.cn; zhifeng.li@siat.ac.cn; yu.qiao@siat.ac.cn).

Z. Zhang is with the Department of Information Engineering, The Chinese University of Hong Kong, Hong Kong (e-mail: zz013@ie.cuhk.edu.hk).

Color versions of one or more of the figures in this letter are available online at http://ieeexplore.ieee.org.

Digital Object Identifier 10.1109/LSP.2016.2603342

cade structure, Mathias et al. [5]–[7] introduce deformable part models for face detection and achieve remarkable performance. However, they are computationally expensive and may usually require expensive annotation in the training stage. Recently, convolutional neural networks (CNNs) achieve remarkable progresses in a variety of computer vision tasks, such as image classification [9] and face recognition [10]. Inspired by the significant successes of deep learning methods in computer vision tasks, several studies utilize deep CNNs for face detection. Yang et al. [11] train deep CNNs for facial attribute recognition to obtain high response in face regions, which further yield candidate windows of faces. However, due to its complex CNN structure, this approach is time costly in practice. Li et al. [19] use cascaded CNNs for face detection, but it requires bounding box calibration from face detection with extra computational expense and ignores the inherent correlation between facial landmarks localization and bounding box regression.

Face alignment also attracts extensive research interests. Research works in this area can be roughly divided into two categories, regression-based methods [12], [13], [16], and template fitting approaches [7], [14], [15]. Recently, Zhang *et al.* [22] proposed to use facial attribute recognition as an auxiliary task to enhance face alignment performance using deep CNN.

However, most of previous face detection and face alignment methods ignore the inherent correlation between these two tasks. Though several existing works attempt to jointly solve them, there are still limitations in these works. For example, Chen *et al.* [18] jointly conduct alignment and detection with random forest using features of pixel value difference. But, these hand-craft features limit its performance a lot. Zhang *et al.* [20] use multitask CNN to improve the accuracy of multiview face detection, but the detection recall is limited by the initial detection window produced by a weak face detector.

On the other hand, mining hard samples in training is critical to strengthen the power of detector. However, traditional hard sample mining usually performs in an offline manner, which significantly increases the manual operations. It is desirable to design an online hard sample mining method for face detection, which is adaptive to the current training status automatically.

In this letter, we propose a new framework to integrate these two tasks using unified cascaded CNNs by multitask learning. The proposed CNNs consist of three stages. In the first stage, it produces candidate windows quickly through a shallow CNN. Then, it refines the windows by rejecting a large number of nonfaces windows through a more complex CNN. Finally, it uses a more powerful CNN to refine the result again and output five facial landmarks positions. Thanks to this multitask learning framework, the performance of the algorithm can be notably improved. The major contributions of this letter are summarized as follows:

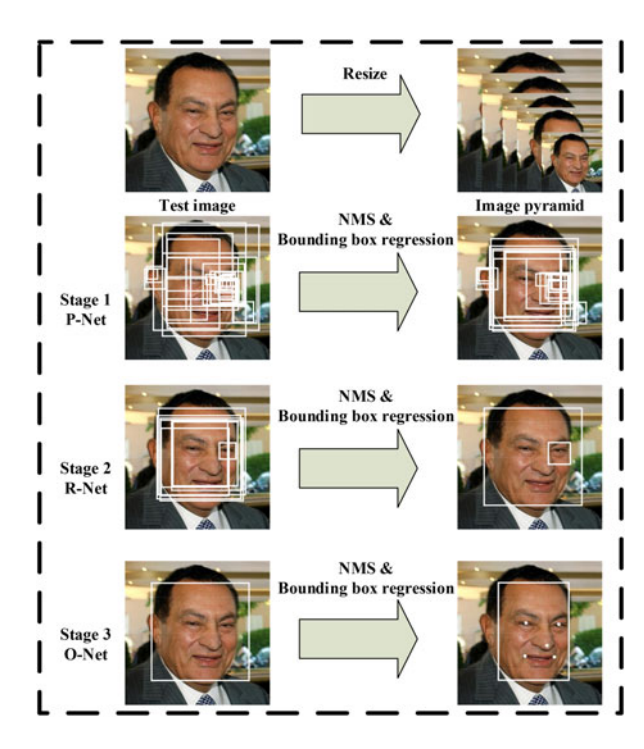


Fig. 1. Pipeline of our cascaded framework that includes three-stage multitask deep convolutional networks. First, candidate windows are produced through a fast P-Net. After that, we refine these candidates in the next stage through a R-Net. In the third stage, the O-Net produces final bounding box and facial landmarks position.

- We propose a new cascaded CNNs-based framework for joint face detection and alignment, and carefully design lightweight CNN architecture for real-time performance.
- 2) We propose an effective method to conduct online hard sample mining to improve the performance.
- 3) Extensive experiments are conducted on challenging benchmarks to show significant performance improvement of the proposed approach compared to the state-of-the-art techniques in both face detection and face alignment tasks.

II. APPROACH

In this section, we will describe our approach toward joint face detection and alignment.

A. Overall Framework

The overall pipeline of our approach is shown in Fig. 1. Given an image, we initially resize it to different scales to build an image pyramid, which is the input of the following three-stage cascaded framework.

Stage 1: We exploit a fully convolutional network, called proposal network (P-Net), to obtain the candidate facial windows and their bounding box regression vectors. Then candidates are calibrated based on the estimated bounding box regression vectors. After that, we employ nonmaximum suppression (NMS) to merge highly overlapped candidates.

Stage 2: All candidates are fed to another CNN, called refine network (R-Net), which further rejects a large number of false candidates, performs calibration with bounding box regression, and conducts NMS.

TABLE I COMPARISON OF SPEED AND VALIDATION ACCURACY OF OUR CNNS AND PREVIOUS CNNS [19]

Group	CNN	$300 \times Forward Propagation$	Validation Accuracy
Group1	12-Net [19]	0.038 s	94.4%
-	P-Net	0.031 s	94.6%
Group2	24-Net [19]	0.738 s	95.1%
-	R-Net	0.458 s	95.4%
Group3	48-Net [19]	3.577 s	93.2%
	O-Net	1.347 s	95.4%

Stage 3: This stage is similar to the second stage, but in this stage we aim to identify face regions with more supervision. In particular, the network will output five facial landmarks' positions.

B. CNN Architectures

In [19], multiple CNNs have been designed for face detection. However, we notice its performance might be limited by the following facts: 1) Some filters in convolution layers lack diversity that may limit their discriminative ability; (2) compared to other multiclass objection detection and classification tasks, face detection is a challenging binary classification task, so it may need less numbers of filters per layer. To this end, we reduce the number of filters and change the 5×5 filter to 3×3 filter to reduce the computing, while increase the depth to get better performance. With these improvements, compared to the previous architecture in [19], we can get better performance with less runtime (the results in training phase are shown in Table I. For fair comparison, we use the same training and validation data in each group). Our CNN architectures are shown in Fig. 2. We apply PReLU [30] as nonlinearity activation function after the convolution and fully connection layers (except output layers).

C. Training

We leverage three tasks to train our CNN detectors: face/nonface classification, bounding box regression, and facial landmark localization.

1) Face Classification: The learning objective is formulated as a two-class classification problem. For each sample x_i , we use the cross-entropy loss as

$$L_i^{\text{det}} = -(y_i^{\text{det}} \log(p_i) + (1 - y_i^{\text{det}})(1 - \log(p_i)))$$
 (1)

where p_i is the probability produced by the network that indicates sample x_i being a face. The notation $y_i^{\text{det}} \in \{0,1\}$ denotes the ground-truth label.

2) Bounding Box Regression: For each candidate window, we predict the offset between it and the nearest ground truth (i.e., the bounding boxes' left, top, height, and width). The learning objective is formulated as a regression problem, and we employ the Euclidean loss for each sample x_i

$$L_i^{\text{box}} = \|\hat{y}_i^{\text{box}} - y_i^{\text{box}}\|_2^2$$
 (2)

where \hat{y}_i^{box} is the regression target obtained from the network and y_i^{box} is the ground-truth coordinate. There are four coordinates, including left top, height and width, and thus $y_i^{\text{box}} \in \mathbb{R}^4$.

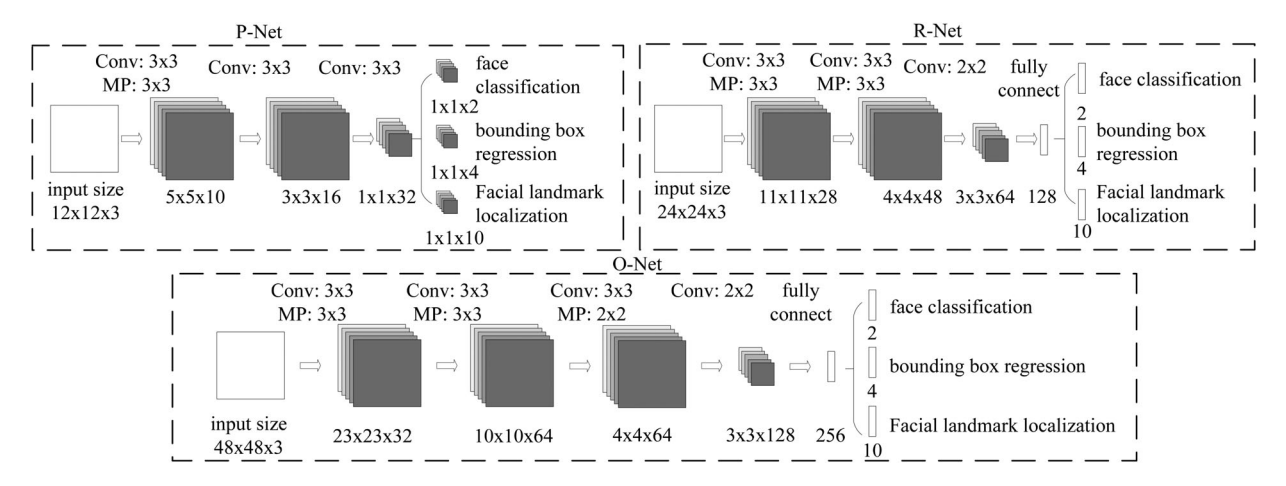


Fig. 2. Architectures of P-Net, R-Net, and O-Net, where "MP" means max pooling and "Conv" means convolution. The step size in convolution and pooling is 1 and 2, respectively.

3) Facial Landmark Localization: Similar to bounding box regression task, facial landmark detection is formulated as a regression problem and we minimize the Euclidean loss as

$$L_i^{\text{landmark}} = \left\| \hat{y}_i^{\text{landmark}} - y_i^{\text{landmark}} \right\|_2^2 \tag{3}$$

where $\hat{y}_i^{\mathrm{landmark}}$ is the facial landmark's coordinates obtained from the network and y_i^{landmark} is the ground-truth coordinate for the ith sample. There are five facial landmarks, including left eye, right eye, nose, left mouth corner, and right mouth corner, and thus $y_i^{\mathrm{landmark}} \in \mathbb{R}^{10}$.

4) Multisource Training: Since we employ different tasks in each CNN, there are different types of training images in the learning process, such as face, nonface, and partially aligned face. In this case, some of the loss functions [i.e., (1)–(3)] are not used. For example, for the sample of background region, we only compute $L_i^{\rm det}$, and the other two losses are set as 0. This can be implemented directly with a sample type indicator. Then, the overall learning target can be formulated as

$$\min \sum_{i=1}^{N} \sum_{j \in \{\text{det,box,landmark}\}} \alpha_{j} \beta_{i}^{j} L_{i}^{j}$$
 (4)

where N is the number of training samples and α_j denotes on the task importance. We use $(\alpha_{\rm det}=1,\alpha_{\rm box}=0.5,\alpha_{\rm landmark}=0.5)$ in P-Net and R-Net, while $(\alpha_{\rm det}=1,\alpha_{\rm box}=0.5,\alpha_{\rm landmark}=1)$ in output network (O-Net) for more accurate facial landmarks localization. $\beta_i^j \in \{0,1\}$ is the sample type indicator. In this case, it is natural to employ stochastic gradient descent to train these CNNs.

5) Online Hard Sample Mining: Different from conducting traditional hard sample mining after original classifier had been trained, we conduct online hard sample mining in face/nonface classification task which is adaptive to the training process.

In particular, in each minibatch, we sort the losses computed in the forward propagation from all samples and select the top 70% of them as hard samples. Then, we only compute the gradients from these hard samples in the backward propagation. That means we ignore the easy samples that are less helpful to strengthen the detector during training. Experiments show that this strategy yields better performance without manual sample selection. Its effectiveness is demonstrated in Section III.

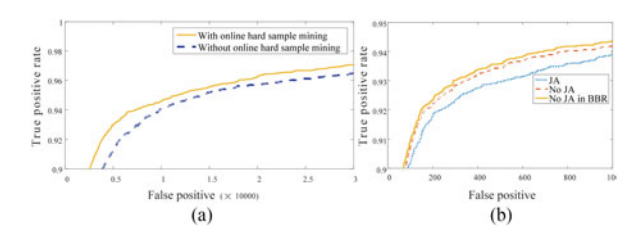


Fig. 3. (a) Detection performance of P-Net with and without online hard sample mining. (b) "JA" denotes joint face alignment learning in O-Net while "No JA" denotes do not joint it. "No JA in BBR" denotes use "No JA" O-Net for bounding box regression.

III. EXPERIMENTS

In this section, we first evaluate the effectiveness of the proposed hard sample mining strategy. Then, we compare our face detector and alignment against the state-of-the-art methods in face detection dataset and benchmark (FDDB) [25], WIDER FACE [24], and annotated facial landmarks in the wild (AFLW) benchmark [8]. FDDB dataset contains the annotations for 5171 faces in a set of 2845 images. WIDER FACE dataset consists of 393 703 labeled face bounding boxes in 32 203 images, where 50% of them for testing (divided into three subsets according to the difficulty of images), 40% for training, and the remaining for validation. AFLW contains the facial landmarks annotations for 24 386 faces and we use the same test subset as [22]. Finally, we evaluate the computational efficiency of our face detector.

A. Training Data

Since we jointly perform face detection and alignment, here we use following four different kinds of data annotation in our training process:

- 1) negatives: regions whose the intersection-over-union (IoU) ratio is less than 0.3 to any ground-truth faces;
- 2) positives: IoU above 0.65 to a ground truth face;
- 3) part faces: IoU between 0.4 and 0.65 to a ground truth face; and
- 4) landmark faces: faces labeled five landmarks' positions.

There is an unclear gap between part faces and negatives, and there are variances among different face annotations. So, we choose IoU gap between 0.3 and 0.4. Negatives and positives are used for face classification tasks, positives and part faces are

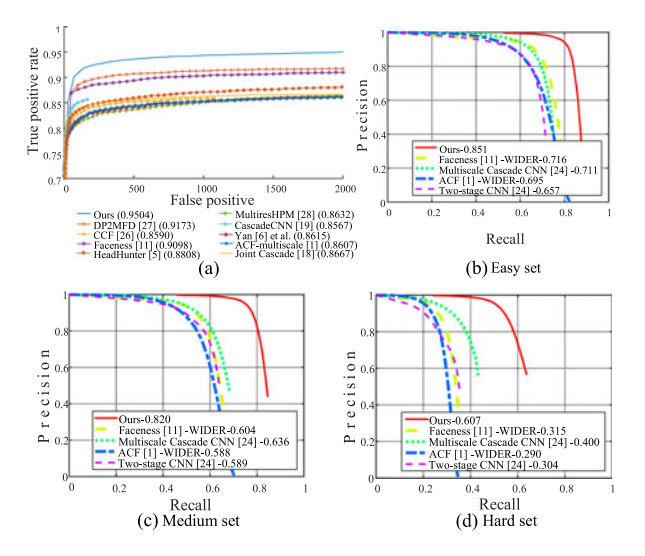


Fig. 4. (a) Evaluation on FDDB. (b)–(d) Evaluation on three subsets of WIDER FACE. The number following the method indicates the average accuracy.

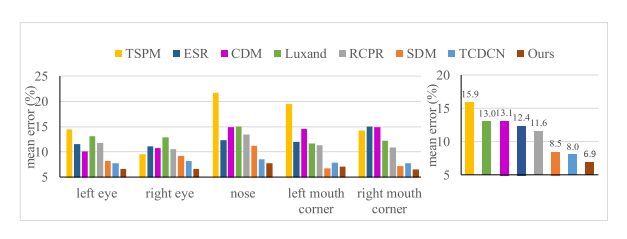


Fig. 5. Evaluation on AFLW for face alignment.

TABLE II SPEED COMPARISON OF OUR METHOD AND OTHER METHODS

Method	GPU	Speed
Ours	Nvidia Titan Black	99 FPS
Cascade CNN [19]	Nvidia Titan Black	100 FPS
Faceness [11]	Nvidia Titan Black	20 FPS
DP2MFD [27]	Nvidia Tesla K20	0.285 FPS

used for bounding box regression, and landmark faces are used for facial landmark localization. Total training data are composed of 3:1:1:2 (negatives/positives/part face/landmark face) data. The training data collection for each network is described as follows:

- 1) P-Net: We randomly crop several patches from WIDER FACE [24] to collect positives, negatives, and part face. Then, we crop faces from CelebA [23] as landmark faces.
- 2) R-Net: We use the first stage of our framework to detect faces from WIDER FACE [24] to collect positives, negatives, and part face while landmark faces are detected from CelebA [23].
- O-Net: Similar to R-Net to collect data, but we use the first two stages of our framework to detect faces and collect data.

B. Effectiveness of Online Hard Sample Mining

To evaluate the contribution of the proposed online hard sample mining strategy, we train two P-Nets (with and without online hard sample mining) and compare their performance on FDDB. Fig. 3(a) shows the results from two different P-Nets on FDDB. It is clear that the online hard sample mining is beneficial to improve performance. It can bring about 1.5% overall performance improvement on FDDB.

C. Effectiveness of Joint Detection and Alignment

To evaluate the contribution of joint detection and alignment, we evaluate the performances of two different O-Nets (joint facial landmarks regression learning and do not joint it) on FDDB (with the same P-Net and R-Net). We also compare the performance of bounding box regression in these two O-Nets. Fig. 3(b) suggests that joint landmark localization task learning help to enhance both face classification and bounding box regression tasks.

D. Evaluation on Face Detection

To evaluate the performance of our face detection method, we compare our method against the state-of-the-art methods [1], [5], [6], [11], [18], [19], [26]–[29] in FDDB, and the state-of-the-art methods [1], [11], [24] in WIDER FACE. Fig. 4(a)–(d) shows that our method consistently outperforms all the compared approaches by a large margin in both the benchmarks. We also evaluate our approach on some challenging photos.¹

E. Evaluation on Face Alignment

In this part, we compare the face alignment performance of our method against the following methods: RCPR [12], TSPM [7], Luxand face SDK [17], ESR [13], CDM [15], SDM [21], and TCDCN [22]. The mean error is measured by the distances between the estimated landmarks and the ground truths, and normalized with respect to the interocular distance. Fig. 5 shows that our method outperforms all the state-of-the-art methods with a margin. It also shows that our method shows less superiority in mouth corner localization. It may result from the small variances of expression, which has a significant influence in mouth corner position, in our training data.

F. Runtime Efficiency

Given the cascade structure, our method can achieve high speed in joint face detection and alignment. We compare our method with the state-of-the-art techniques on GPU and the results are shown in Table II. It is noted that our current implementation is based on unoptimized MATLAB codes.

IV. CONCLUSION

In this letter, we have proposed a multitask cascaded CNNs-based framework for joint face detection and alignment. Experimental results demonstrated that our methods consistently outperform the state-of-the-art methods across several challenging benchmarks (including FDDB and WIDER FACE benchmarks for face detection, and AFLW benchmark for face alignment) while achieves real-time performance for 640 \times 480 VGA images with 20 \times 20 minimum face size. The three main contributions for performance improvement are carefully designed cascaded CNNs architecture, online hard sample mining strategy, and joint face alignment learning.

¹Examples are shown in http://kpzhang93.github.io/SPL/index.html

REFERENCES

- B. Yang, J. Yan, Z. Lei, and S. Z. Li, "Aggregate channel features for multi-view face detection," in *IEEE Int. Joint Conf. Biometrics*, 2014, pp. 1–8.
- [2] P. Viola and M. J. Jones, "Robust real-time face detection," Int. J. Comput. Vis., vol. 57, no. 2, pp. 137–154, 2004.
- [3] M. T. Pham, Y. Gao, V. D. D. Hoang, and T. J. Cham, "Fast polygonal integration and its application in extending Haar-like features to improve object detection," in *IEEE Conf. Comput. Vis. Pattern Recognit.*, 2010, pp. 942–949.
- [4] Q. Zhu, M. C. Yeh, K. T. Cheng, and S. Avidan, "Fast human detection using a cascade of histograms of oriented gradients," in *IEEE Comput. Conf. Comput. Vis. Pattern Recognit.*, 2006, pp. 1491–1498.
- [5] M. Mathias, R. Benenson, M. Pedersoli, and L. Van Gool, "Face detection without bells and whistles," in *Eur. Conf. Comput Vis.*, 2014, pp. 720–735.
- [6] J. Yan, Z. Lei, L. Wen, and S. Li, "The fastest deformable part model for object detection," in *IEEE Conf. Comput. Vis. Pattern Recognit.*, 2014, pp. 2497–2504.
- [7] X. Zhu and D. Ramanan, "Face detection, pose estimation, and landmark localization in the wild," in *IEEE Conf. Comput. Vis. Pattern Recognit.*, 2012, pp. 2879–2886.
- [8] M. Köstinger, P. Wohlhart, P. M. Roth, and H. Bischof, "Annotated facial landmarks in the wild: A large-scale, real-world database for facial landmark localization," in *IEEE Conf. Comput. Vis. Pattern Recognit. Workshops*, 2011, pp. 2144–2151.
- [9] A. Krizhevsky, I. Sutskever, and G. E. Hinton, "ImageNet classification with deep convolutional neural networks," in *Adv. Neural Inf. Process.* Syst., 2012, pp. 1097–1105.
- [10] Y. Sun, Y. Chen, X. Wang, and X. Tang, "Deep learning face representation by joint identification-verification," in *Adv. Neural Inf. Process. Syst.*, 2014, pp. 1988–1996.
- [11] S. Yang, P. Luo, C. C. Loy, and X. Tang, "From facial parts responses to face detection: A deep learning approach," in *IEEE Int. Conf. Comput. Vis.*, 2015, pp. 3676–3684.
- [12] X. P. Burgos-Artizzu, P. Perona, and P. Dollar, "Robust face landmark estimation under occlusion," in *IEEE Int. Conf. Comput. Vis.*, 2013, pp. 1513–1520.
- [13] X. Cao, Y. Wei, F. Wen, and J. Sun, "Face alignment by explicit shape regression," Int. J. Comput. Vis., vol. 107, no. 2, pp. 177–190, 2012.
- [14] T. F. Cootes, G. J. Edwards, and C. J. Taylor, "Active appearance models," *IEEE Trans. Pattern Anal. Mach. Intell.*, vol. 23, no. 6, pp. 681–685, Jun. 2001.

- [15] X. Yu, J. Huang, S. Zhang, W. Yan, and D. Metaxas, "Pose-free facial landmark fitting via optimized part mixtures and cascaded deformable shape model," in *IEEE Int. Conf. Comput. Vis.*, 2013, pp. 1944–1951.
- [16] J. Zhang, S. Shan, M. Kan, and X. Chen, "Coarse-to-fine auto-encoder networks (CFAN) for real-time face alignment," in *Eur. Conf. Comput. Vis.*, 2014, pp. 1–16.
- [17] Luxand Incorporated: Luxand face SDK. [Online]. Available: http://www.luxand.com/
- [18] D. Chen, S. Ren, Y. Wei, X. Cao, and J. Sun, "Joint cascade face detection and alignment," in Eur. Conf. Comput. Vis., 2014, pp. 109–122.
- [19] H. Li, Z. Lin, X. Shen, J. Brandt, and G. Hua, "A convolutional neural network cascade for face detection," in *IEEE Conf. Comput. Vis. Pattern Recognit.*, 2015, pp. 5325–5334.
- [20] C. Zhang and Z. Zhang, "Improving multiview face detection with multitask deep convolutional neural networks," in *IEEE Winter Conf. Appl. Comput. Vis.*, 2014, pp. 1036–1041.
- [21] X. Xiong and F. Torre, "Supervised descent method and its applications to face alignment," in *IEEE Conf. Comput. Vis. Pattern Recognit.*, 2013, pp. 532–539.
- [22] Z. Zhang, P. Luo, C. C. Loy, and X. Tang, "Facial landmark detection by deep multi-task learning," in *Eur. Conf. Comput. Vis.*, 2014, pp. 94–108.
- [23] Z. Liu, P. Luo, X. Wang, and X. Tang, "Deep learning face attributes in the wild," in *IEEE Int. Conf. Comput. Vis.*, 2015, pp. 3730–3738.
- [24] S. Yang, P. Luo, C. C. Loy, and X. Tang, "WIDER FACE: A Face detection benchmark," arXiv:1511.06523.
- [25] V. Jain and E. G. Learned-Miller, "FDDB: A benchmark for face detection in unconstrained settings," Univ. Massachusetts, Amherst, MA, USA, Tech. Rep. UMCS-2010-009, 2010.
- [26] B. Yang, J. Yan, Z. Lei, and S. Z. Li, "Convolutional channel features," in IEEE Int. Conf. Comput. Vis., 2015, pp. 82–90.
- [27] R. Ranjan, V. M. Patel, and R. Chellappa, "A deep pyramid deformable part model for face detection," in *IEEE Int. Conf. Biometrics Theory, Appl.* Syst., 2015, pp. 1–8.
- [28] G. Ghiasi and C. C. Fowlkes, "Occlusion coherence: Detecting and localizing occluded faces," arXiv:1506.08347.
- [29] S. S. Farfade, M. J. Saberian, and L. J. Li, "Multi-view face detection using deep convolutional neural networks," in ACM Int. Conf. Multimedia Retrieval, 2015, pp. 643–650.
- [30] K. He, X. Zhang, S. Ren, and J. Sun, "Delving deep into rectifiers: Surpassing human-level performance on ImageNet classification," in *IEEE Int. Conf. Comput. Vis.*, 2015, pp. 1026–1034.